Modelling the seasonal dynamics of marine plankton in the southern Baltic Sea. Part 2. Numerical simulations*

OCEANOLOGIA, 48 (1), 2006.
pp. 41–71.

KEYWORDS
Nutrients
Phytoplankton
Microzooplankton
Pseudocalanus elongatus
Clupea harengus
Baltic Sea
Turbulence
Encounter rate

Lidia Dzierzbicka-Głowacka

Institute of Oceanology,
Polish Academy of Sciences,
Powstańców Warszawy 55, PL–81–712 Sopot, Poland;

e-mail: dzierzb@iopan.gda.pl

Received 12 September 2005, revised 20 February 2006, accepted 24 February 2006.

Abstract

This work presents numerical simulations of the time-dependent vertical distributions of phytoplankton, microzooplankton, *Pseudocalanus elongatus*, early juvenile herring (*Clupea harengus*) and two nutrient components (total inorganic nitrogen and phosphate) using the 1*D*-Coupled Ecosystem Model with a high-resolution mesozooplankton (herbivorous copepods) module for *P.elongatus* and a simple prey-predator model for early juvenile herring *C. harengus*. This model was discussed in detail in Part 1. The calculations were done for one year (1999) for a station in the Gdańsk Deep (southern Baltic Sea). The results of the simulations were compared with the mean concentrations of nutrients, phytoplankton and zooplankton recorded *in situ*. The differences between the calculated and mean recorded values of nutrients and phytoplankton are c. 5–30% and depend on the month and depth for which the calculations were done. However, the calculated depth-integrated biomass of *P. elongatus* differs from the mean recorded value.

* This research was carried out as part of the statutory programme of the Institute of Oceanology in Sopot, Poland (No II.1.4) and was funded by the Polish State Committee of Scientific Research (grant No 2P04F 075 27, 2004–2006).

This difference ranges from 30 to 50% at the end of May. The 1DCEM model can be used to forecast ecological changes in the southern Baltic Sea.

1. Introduction

Part 2 of this paper discusses the testing of the one-dimensional Coupled Ecosystem Model, described in Part 1 (Dzierzbicka-Głowacka 2005b). The 1DCEM was used to simulate temporal changes in the vertical distributions of nutrients (total inorganic nitrogen and phosphate), phytoplankton carbon, microzooplankton, mesozooplankton (*Pseudocalanus elongatus*) and early juvenile herring *Clupea harengus*. These numerical simulations were done for one station in the Gdańsk Deep (southern Baltic Sea) and for one particular year (1999). Since the outputs of the meteorological submodel were obtained using meteorological data for 1999, the numerical results were compared with the mean values of empirical data for 1999 taken from the literature.

The model consists of three submodels – meteorological, physical and biological: the meteorological component drives both 1D models, and the output of the physical model is also used for driving the biological model. With a copepod model and a simple prey-predator model, the biological model consists of seven mass conservation equations. There are six diffusion-type, partial second-order differential equations for phytoplankton, microzooplankton, mesozooplankton and early juvenile fish, as well as two nutrient components (total inorganic nitrogen and phosphate). The seventh equation, an ordinary differential equation, describes the development of detritus at the bottom.

Phytoplankton is modelled with the aid of only one state variable and is taken to be a dynamically passive physical quantity (i.e. it is incapable of making autonomous movements).

Nutrients are represented by two components: total inorganic nitrogen (NO_3 + NO_2 + NH_4) and phosphate (PO_4). The nutrient serves as both the trigger and limiting agent for primary production.

One state variable for microzooplankton is considered. This is defined as heterotrophic planktonic organisms from 10 to 500 μm SED, excluding heterotrophic nanoflagellates and the naupliar/larval stages of larger zooplankton and of benthic organisms. The microzooplankton consists of ciliates and other heterotrophic protests filter-feeding on phytoplankton.

The mesozooplankton (herbivorous copepods) is represented by one species of *P. elongatus* for stages C1 to adult. The population is composed of six cohorts of the different developmental stages; the assumption is therefore that the next generation is recruited after a certain period of adult life. This period, during which the next generation is recruited, starts when an

individual reaches the adult stage and ends when the new generation arrives on the scene, that is, when the eggs are laid. The egg laying pattern can be approximated to the concept of a single brood.

According to the definition of microzooplankton, this also consists of *P. elongatus* – for stages from the egg to N6 (nauplius). This model assumes that when *Pseudocalanus* reaches a weight of 0.1 μgC, it is then classified as mesozooplankton.

The predator is represented by 3 cohorts of early juvenile herring *C. harengus* of the 4–10 cm size class, whose growth rate is controlled by the encounter rate between consumer and prey. The concept of the detrital pool at the bottom has been introduced to create a time-lag between the remineralisation of most of the detritus and the eventual replenishment of the upper layer with nutrients. This complex process is parameterised by assuming a net remineralisation rate for bottom detritus.

The phytoplankton standing stock, zooplankton, early juvenile fish and nutrients in the water column serve as time- and depth-dependent pools. Detritus is a time-dependent pool at the bottom. All pools are prognostic state variables. Bacteria are not explicitly simulated as prognostic variables. Their activity only appears implicitly in the parameterisations of the remineralisation terms. Benthic detritus accumulates by sinking out of the water column. It is regenerated by bacterial action, and the resulting nutrients move upwards by turbulent diffusion.

In Part 1, section 2 described the combined marine ecosystem model, and subsection 2.1 presented the concept of the model. The three components of 1*D*CEM involving the biology, physics and meteorology together with the boundary and initial conditions were presented in 2.2, 2.3 and 2.4 respectively. In Part 2, the sections cover the following aspects of the paper: section 2 – forcing functions; section 3 –input data for the simulation studies; section 4 – the numerical results; section 5 – comparison of the experimental data with the simulations; section 6 – discussion.

2. The forcing functions

For the physical submodel, the wind stress, heat and radiative fluxes at the sea surface are needed and are determined from standard meteorological components for a point over the Gdańsk Deep. The local thermal energy flux consists of the global radiation Q_g, long-wave back radiation Q_B, sensible heat flux Q_S and latent heat flux Q_L. The global radiation is calculated using the a radiation model described by Rozwadowska & Isemer (1998) (see eq. (68) in Part 1). The other heat fluxes, Q_B, Q_S, Q_L, enter the physical system via the surface boundary conditions. The long-wave back radiation Q_B is calculated by eq. (69) from the formula of Zapadka et al. (2001).

Sensible and latent heat fluxes Q_S and Q_L take place by turbulent transfer, calculated using Launiainen's (1979) formulae (see eqs. (70) and (71) in Part 1). The formulae for wind stress are taken from Lehmann (1995) (see eqs. (65) and (66) in Part 1). All these formulae were presented in detail in Part 1.

The study period, which started in January 1999, was preceded by a relatively cold early December and warm late December. In January 1999 (Fig. 1a), higher than normal temperatures were brought in by southerly and westerly air masses from the Atlantic. The mean January air temperature was higher by c. 5°C than the long-term mean for 1961–90. February was slightly colder, although still above the norm. In autumn, there was a flow of warmer air masses from the west, resulting in a relatively warm December, with temperatures from 7°C to −3°C. Hence, the air temperature was higher than the mean values for autumn and winter, except for a few days in the second half of October and in November, when the temperature fell to c. 7°C below the average. Air temperatures in the other months were similar to or slightly higher than the long-term means. In the winter and autumn, winds were quite strong, especially in February, October and December (Fig. 1b). In 1999 there were severe storms in early February and late November, when wind velocities reached c. 20°. At the beginning of January a depression bringing cold air masses mostly from the west and north caused a drop in the temperature.

There were noticeable differences in global radiation (Q_g) in 1999: the sun shone strongly in March and May, radiation was very low in the first half of April, the second half of June and the first half of August. Having calculated the separate heat and radiative fluxes, we can estimate the mean daily heat balance at the surface. In comparison with the other heat fluxes, the global radiation Q_g is the most important parameter. The long-wave back radiation Q_B is rather stable throughout the year. The effect of the latent Q_L and sensible Q_S heat fluxes on the heat balance at the surface Q is visible in the temporal distributions Q, even though it is they are the smallest. The annual cycles of the daily heat balances Q and global radiation Q_g are shown in Fig. 2. Negative values of Q were registered in January–February and October–December with minima in January and December. However, values of Q were positive from mid-March to October with the maximum in July–August. Q values change from negative to positive in mid-March, and from positive back to negative at the end of September. During these two latter periods, the temperature of the upper layer reaches extreme values and the heat content scarcely changes – this is typical of periods when the sea is in thermal balance. The positive values of Q in the warm seasons of the year are described almost exclusively by the ratio of the global radiation

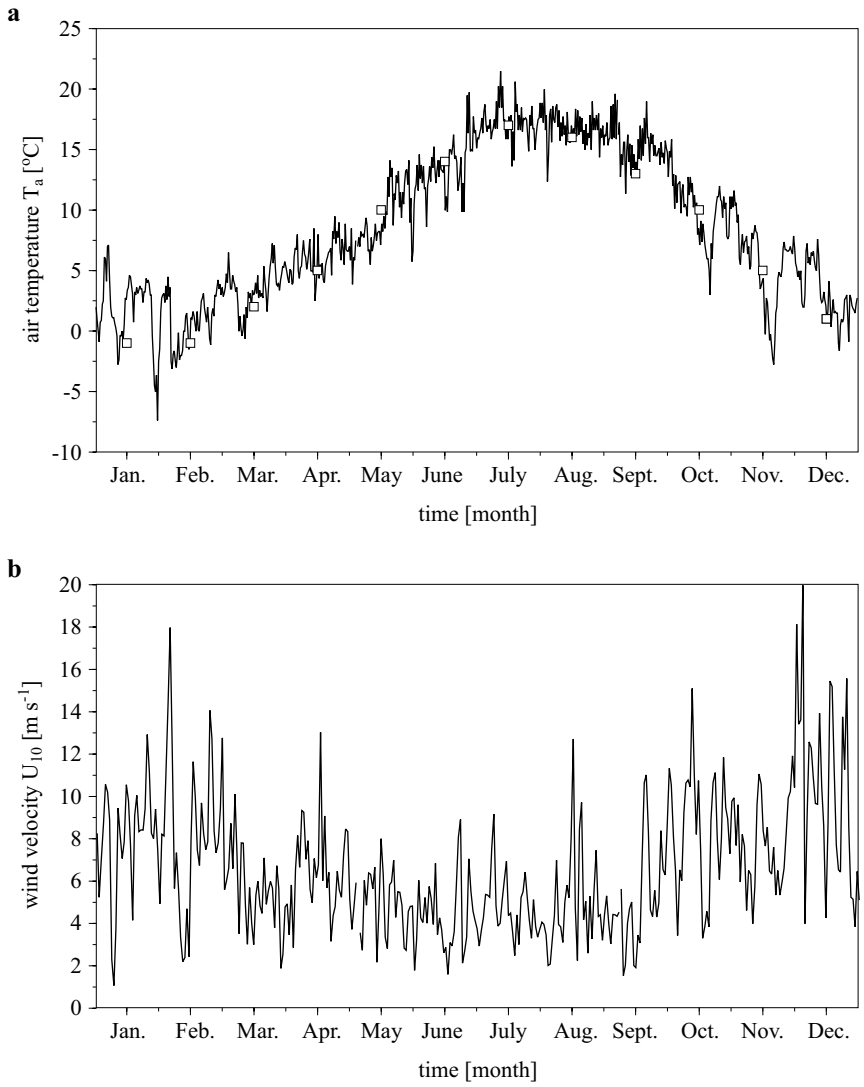

Fig. 1. Air temperature (a) and mean daily wind velocity (b) at the Gdańsk Deep in 1999. Long-term means for 1961–1990 (according to data of the Institute of Meteorology and Water Management)

Q_g to the long-wave back radiation Q_B; the sensible and latent heat fluxes (Q_S and Q_L) at these times are low. The daily heat balance varies from -200 to 100 W m^{-2} in winter and from 0 to 360 W m^{-2} in summer. The seasonal thermocline begins to establish itself once the heat balance at the sea surface becomes persistently positive. In Fig. 2a we see that the envelope of daily heat balance observations intersects the zero line for about half the month of March. This gives us the time it takes for the seasonal thermocline

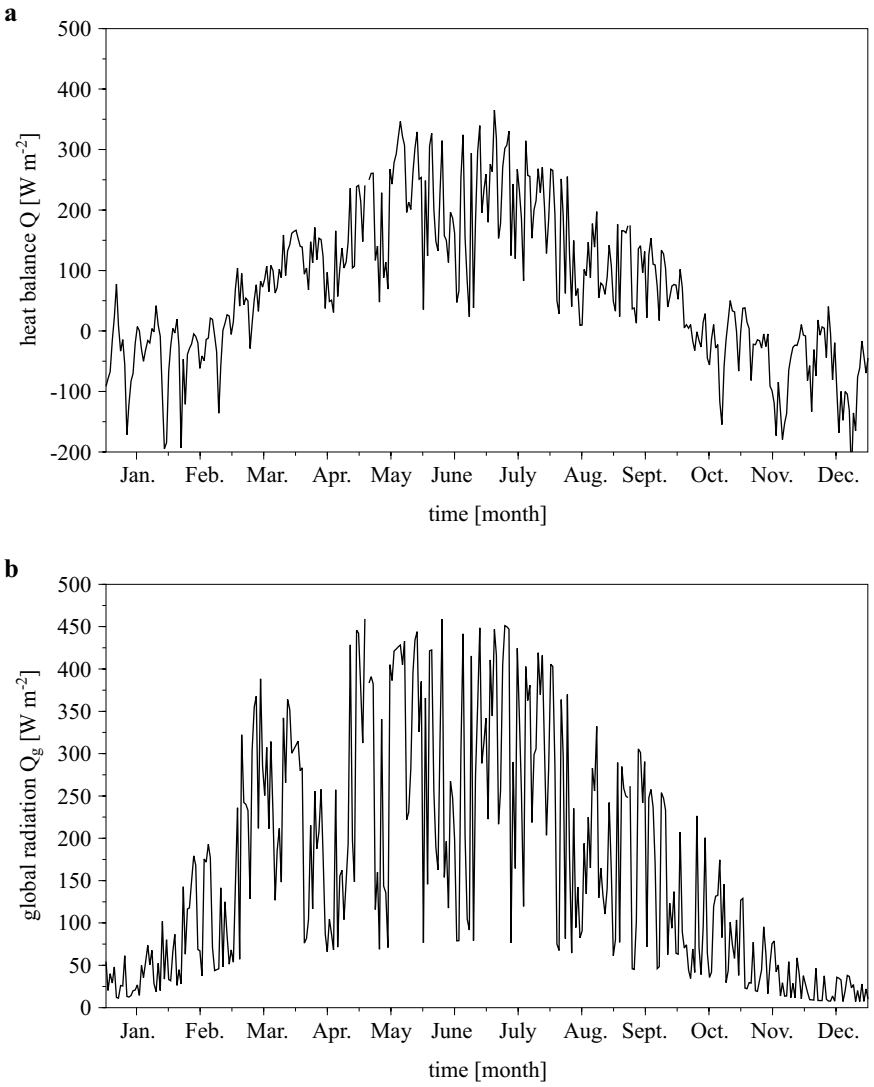

Fig. 2. Daily heat balance at the sea surface (a) and daily global radiation (b) in the Gdańsk Deep in 1999

to become established. Oceanographic forcing is needed in the biological production model. Firstly, time- and space-dependent turbulent diffusion rates resulting from the simulation of the physical upper layer dynamics are introduced into the biological upper layer model by the diffusion term. Secondly, the photosynthetically available radiation (PAR) at the sea surface E_o ($E_o(t) = \varepsilon Q_g$) is identified as ε ($\varepsilon = 0.465(1.195 - 0.195\,T_{cl})$) where T_{cl} is the cloud transmittance function (Czyszek et al. 1979) of the net flux of short-wave radiation Q_g from eq. (68). Photosynthesis is regulated by

the light limitation factor from eq. (13), which is supplied with underwater light calculated by eq. (16). The global radiation Q_g enters the source term (primary production) in the phytoplankton equation eq. (3) and the temperature equation eq. (60).

The temperature field controls primary production and respiration, as described in eqs. (14), (15) and (20). The turbulent diffusion rate resulting from the simulation of the physical upper layer dynamics from eq. (11) is introduced into the biological upper layer model.

Closing the system towards the upper trophic levels is the hardest task. There are at least two possible ways of doing this. For one thing, an equation could be added to account for larger species, with an ingestion term describing predation on larval fish. At first sight this would seem to be a good solution; however, it necessitates the introduction of an expression for the predation of larval fish by larger carnivores, and so merely shifts the problem to a higher order. For another, we can describe predation on early juvenile herring (eq. (10)) on the basis of the increase in their biomass on the assumption that the incurred loss is proportional to a coefficient α. This has the advantage that no additional partial differential equation is needed.

3. Input data

The dynamic constants used in the biological and physical model were determined from literature data; they are listed in Tables 1 and 2 (see Appendix, p. 69). The values of the parameters were chosen reasonably close to Baltic levels.

The following assumptions were made in the calculation:

1. The initial phytoplankton biomass ($Phyt$ = 0.01 mgC m^{-3}) and inorganic nitrogen ($Nutr_N$ =6 mmol m^{-3}) and phosphate ($Nutr_P$ = 0.6 mmol m^{-3}) concentrations, were assumed to be constant with depth and to be the mean values of empirical data for the Gdańsk Deep (Witek et al. 1993, IMGW 2000).

2. The initial microzooplankton biomass was obtained according to data by Witek (1995) as Z_{micro} = 0.1 mgC m^{-3} with a maximum growth rate of 0.17 d^{-1}. The maximum growth rate of ciliates was 0.4 d^{-1}, that of heterotrophic dinoflagellates was three times lower (Witek 1995). However, for copepod nauplii, it was taken to be the mean value for two copepods: *Acartia* spp. and *Temora longicornis*.

3. Represented by passive particles, the microzooplankton is assumed to be speedless. This is not realistic, but its speed is indeed very, very

small – c. 0.5 body length. Hence, the speed of microzooplankton is assumed to be zero.

4. The mean weights for specific development stages of *P. elongatus* were assumed after standard HELCOM data (Hernroth (ed.) 1985) for the Gdańsk Deep; the initial population of *P. elongatus* had no eggs and no nauplii N1-N6, 550 C1, 450 C2, 350 C3, 250 C4, 150 C5, and 90 adults m^{-2}, giving a total biomass of c. 1.2 mgC m^{-2} in the upper 30 m layer, and 1800 C1, 1500 C2, 900 C3, 600 C4, 400 C5, and 200 adults m^{-2}, giving a total biomass of c. 3 mgC m^{-2} in the lower 40 m layer; these data are based on empirical data supplied by Witek (1995) and L. Bielecka (personal communication).

5. Swimming speed of *P. elongatus* adults, u, was 4.31 ± 1.65 cm s^{-1} after Viitasalo et al. (2001); however, for copepodids, u was based on the estimates of Sundby & Fossum (1990), who used an average speed of 0.5 body length.

6. During the first half of the year the predator biomass $B = 0$ and the initial predator biomass was $B = B_1 = 48$ $mg_{d.w.}$ m^{-3} of the 1st cohort at the end of June, plus $B_2 = 36$ $mg_{d.w.}$ m^{-3} of the 2nd cohort at the end of July and plus $B_3 = 24$ $mg_{d.w.}$ m^{-3} of the 3rd cohort at the end of August; these values were obtained after Margoński (2000) and Fey (2001). A factor of 0.6 was used here to convert from ash-free dry weight to mg carbon.

7. The average weight-specific growth rates of herring larvae fed at high and low prey levels were relatively constant at about 7% d^{-1} and 1.5% d^{-1}, respectively (after Johannessen et al. 2000). Predator growth parameters g_1 and g_2 were chosen such that the growth rate ranged from $0 < g < g_{\max}$, where g_1 is the proportionality parameter between growth rate and encounter rate and g_2 is the constant growth rate term.

8. High survival rates (85–92%) of herring larvae were observed by Johannessen et al. (2000) at high prey levels with daily mean mortality rates less than 0.4%. At low prey levels, 43–49% of the larvae survived yielding mean mortality rates of 1.5–2.4% d^{-1}.

The conversions from total inorganic nitrogen and phosphate to carbon, applied in the equations for nutrients as $g_N = 0.0167$ mmol N$(\text{mgC})^{-1}$ and $g_P = 0.612 \times 10^{-3}$ mmol P$(\text{mgC})^{-1}$, are given in Table 1 (see Appendix p. 69).

The results of the numerical simulations described in section 5 are compared with the mean observed values assuming:

– for phytoplankton, the C/Chl a ratio to be the mean value for the southern Baltic Sea in the upper layer after Witek et al. (1993) (discussion – see section 5);

– for microzooplankton, organic carbon content of $gC/g_{w.w.} = 0.11$ (Edler (ed.) 1979) for ciliates and $gC/g_{w.w.} = 0.13$ for heterotrophic dinoflagellates;

– for *P. elongatus*, organic carbon content $gC/g_{w.w} = 0.064$ (Vinogradov & Shushkina 1987).

Comment

Spring spawning herring stocks normally occur as components of the pelagic fish community in the Baltic Sea and adjacent waters. The Vistula Lagoon is an important spawning area for southern Baltic spring-spawning herring *C. harengus*. At the turn of winter and spring (in March), adults migrate from the southern Baltic to the spawning area in the shallow, brackish water of the Vistula Lagoon (Fey 2001). Herring in the Vistula Lagoon has three cohorts each year (Margoński 2000). In 1999 the of larvae abundance in the Vistula Lagoon was 495–128 individuals in 100 m^3. Herring larvae ($>$ 5 mm long) appeared in plankton samples during the very first cruise in 1999, at the beginning of April (07 April). When young herring are about 40 to 50 mm long they metamorphose, developing the morphological characteristics of adults; they are then identified as juveniles. In laboratory studies, metamorphosis took about 10 days to complete at 15°C (Blaxter & Holliday 1963). In the Vistula Lagoon metamorphosis begins in June. Early juvenile herring of the first cohort emigrated from the Polish part of the Vistula Lagoon at the end of June, the second cohort in July, and the third cohort in August. Early juveniles (c. 40 mm) appear in the Gulf of Gdańsk two weeks later, assuming that its speed is c. 4 cm s^{-1} (after Miller et al. 1988).

Juvenile herring feed on a variety of zooplankton; copepods are the most important prey throughout the year. Feeding studies of fish larvae have shown that *Pseudocalanus*, *Acartia*, *Temora* nauplii and copepodid stages are important dietary components of a number of different fish species in the Baltic Sea and adjacent waters. The copepod *Pseudocalanus* is one of the more abundant zooplankton species in these waters.

4. Results

In order to explore meteorologically-induced biological variability, the numerical simulations were performed with the combined meteorological-

physical-biological model for one single annual cycle of meteorological forcing.

Primary production and respiration were calculated on the basis of modelled temperature fields from the physical model (as the output). Fig. 3a shows the temperature distributions at this station in the Gdańsk Deep in

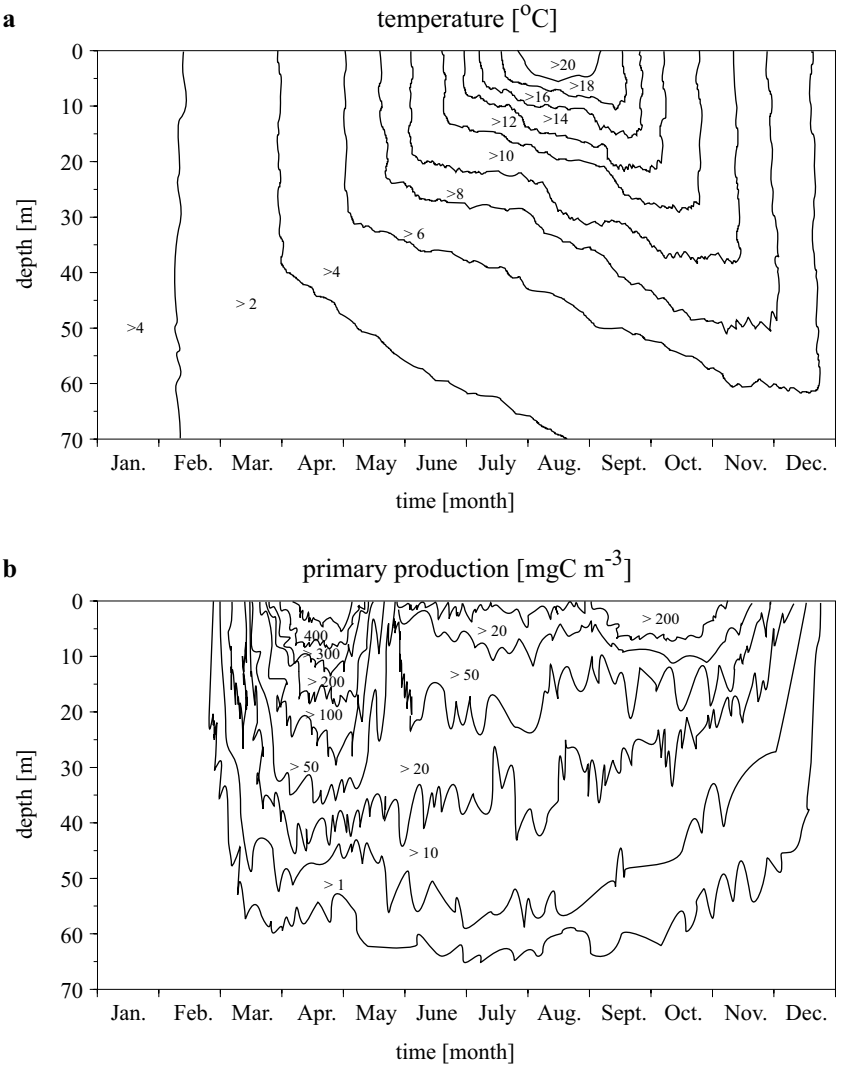

Fig. 3. Annual simulation. Simulated profiles of temperature (a), primary production (b), phytoplankton (c), nutrients – phosphate (d) and total inorganic nitrogen (e), microzooplankton (f), mesozooplankton – *Pseudocalanus elongatus* (g) and early juvenile herring *Clupea harengus* (h) in the Gdańsk Deep in 1999

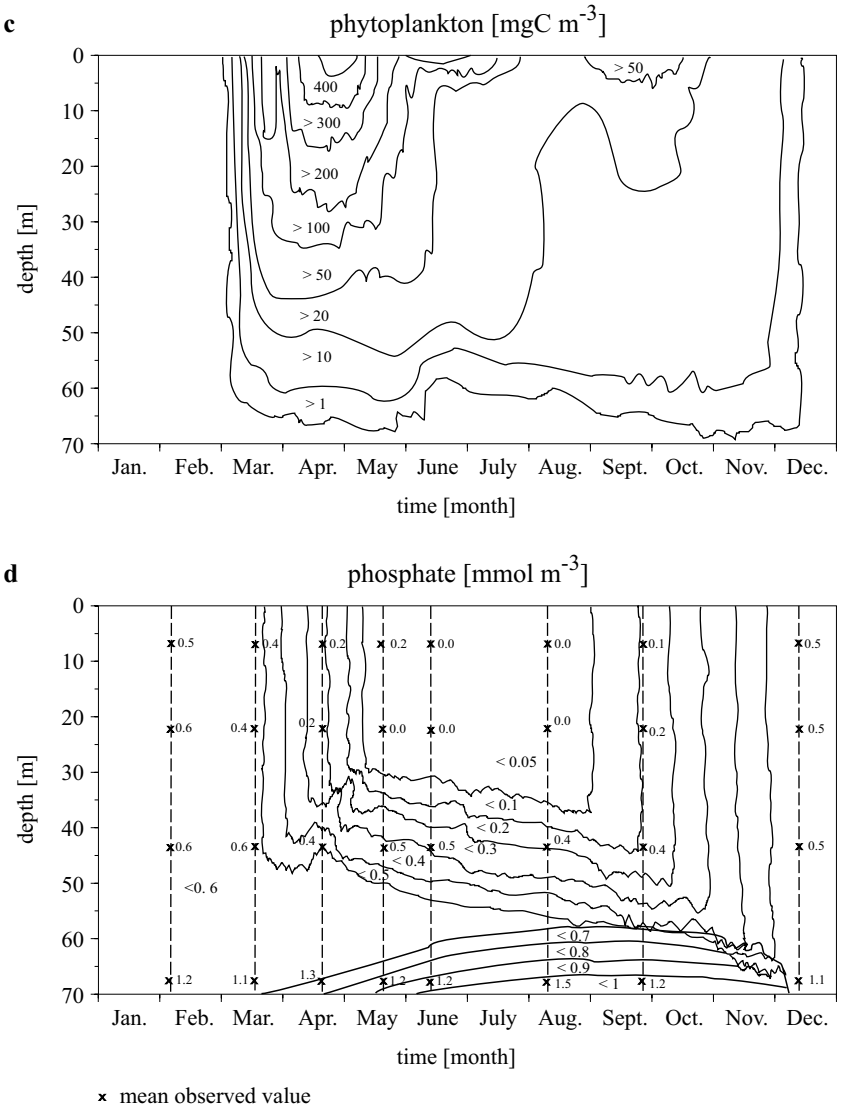

Fig. 3. (*continued*)

the southern Baltic Sea. In 1999, a period of 231 days elapsed between the surfacing of the 6°C isopleth in spring and its disappearance in autumn; it lay in the 30–60 m depth range. From day 186 to day 268 the water temperature was > (16°C) down to 5–20 m. The thermocline began to disappear on day 352 in the late autumn; c. three months (84 days) elapsed between the surfacing of the 16°C isotherm and the surfacing of the 6°C isotherm in the autumn on days 268 and 352 respectively. The maximum water temperature was c. 21°C in August.

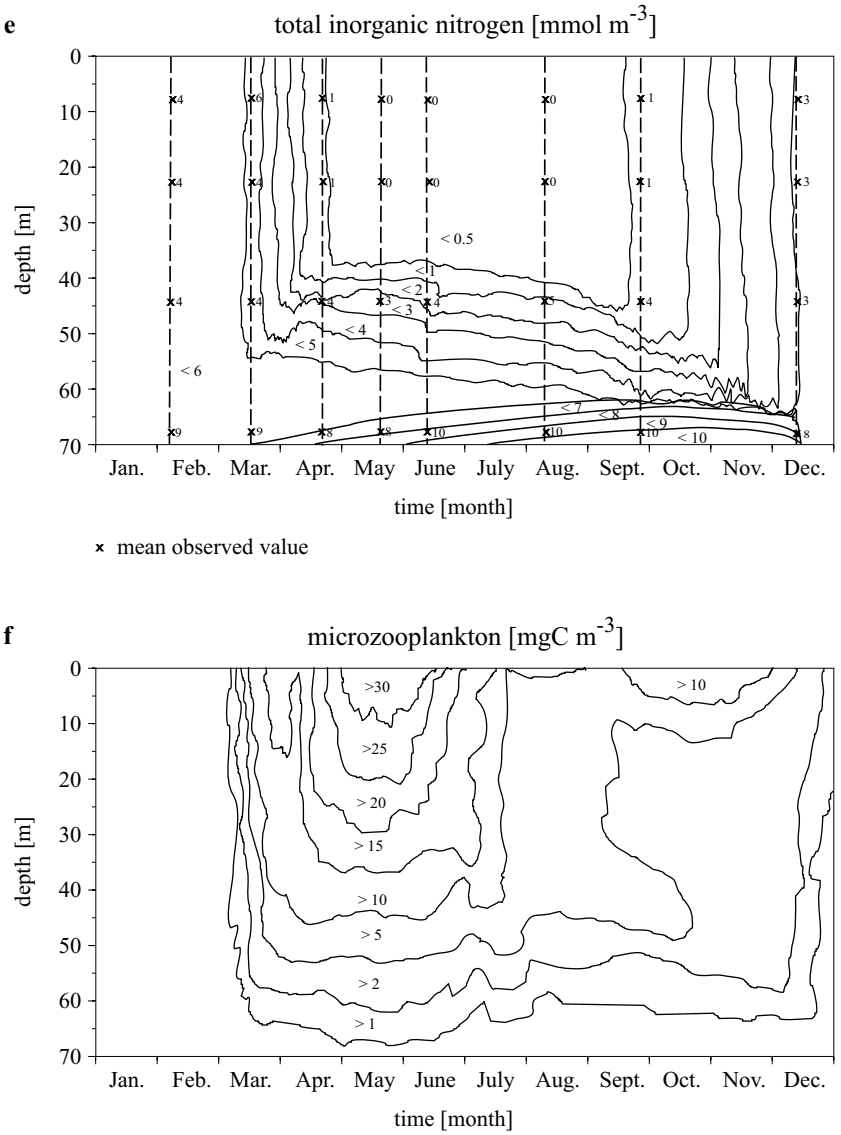

Fig. 3. (*continued*)

The biological simulation produced time series of profiles for the state variables $Phyt$, $Nutr_N$, $Nutr_P$, Z_{micro}, Z_{meso} and B and time series for benthic detritus $Detr$ (see eqs. (1)–(10) in Part 1.). Fig. 3b shows the distributions of gross primary production during the year.

Primary production > 200 mgC m^{-3} took place between days 79 and 134, the highest values being recorded in April. Large values were also recorded between July and October. Primary production was more intense

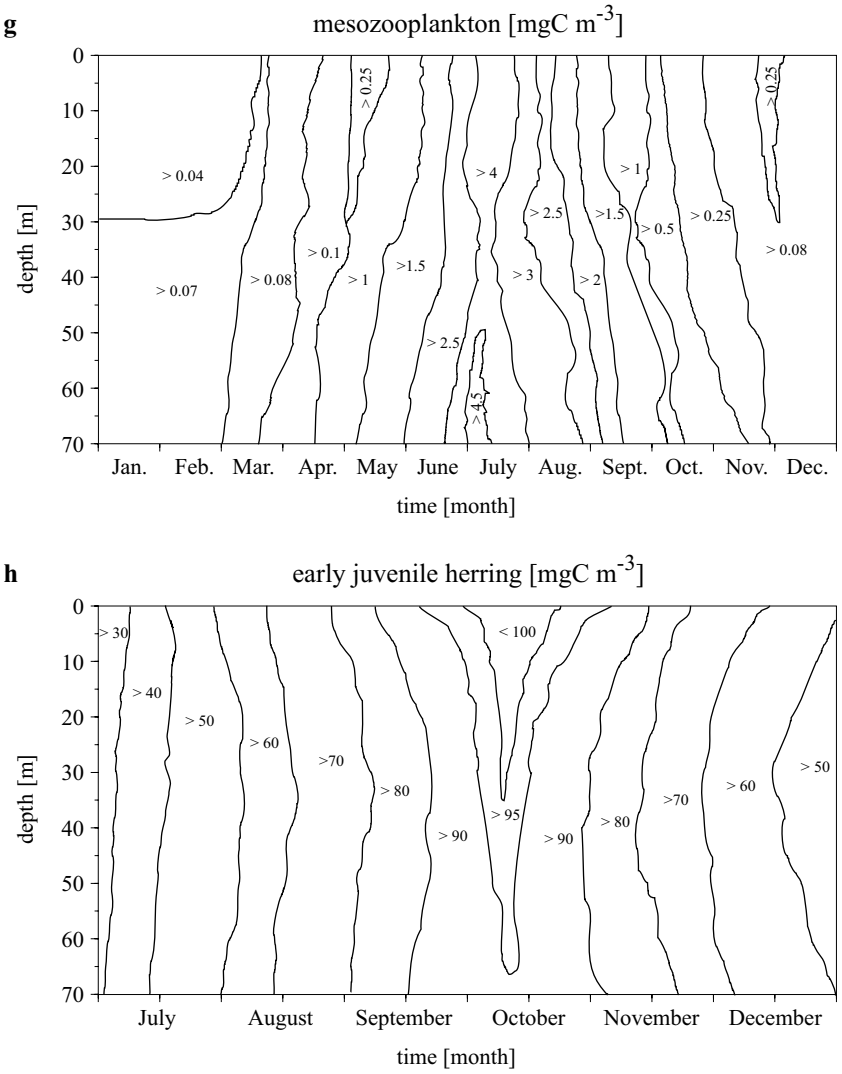

Fig. 3. (*continued*)

during periods of greater insolation. What was puzzling was the relatively low primary production during the early spring bloom. It is true that during this period the biomass of zooplankton is still very low, so phytoplankton grazing is at a minimum. But under these conditions the algal biomass may increase at lower intensities of primary production than during later periods. From June to September primary production took place at greater depths, its position always being where the balance of light and nutrient availability was favourable. The spring bloom displayed a subsurface maximum, a little below 20 m.

The distributions of primary production were reflected by the concentrations of phytoplankton biomass (Fig. 3c) and nutrients (phosphate and total inorganic nitrogen Figs 3d and 3e). The spring bloom was probably triggered in the first half of March. It is initiated by the heating event and the extremely low winds in mid-March.

The end of the permanent overturning of the water in mid-March is the main event allowing the phytoplankton to start growing, according to Sverdrup's (1953) theory. The depths of the upper layer, which are determined by the mixing intensity in the water column, show that strong gradients develop in the nutrient concentration. By late April inorganic nitrogen in the upper 40 m had become depleted to a concentration of < 0.5 mmol m^{-3}; phosphate became similarly depleted to a concentration of < 0.05 mmol m^{-3}, but three weeks later. The deepening of the isotherms occurs faster than the deepening of the isopleths for nutrients, because of the counteracting upward diffusion of nutrients from the bottom source. From spring to autumn the deepening events for the nutricline correspond directly to the deepening events of the mixed layer caused by wind events. A strong spring bloom leads to relatively high quantities of detrital material sinking to the bottom early enough in the year for the process of remineralisation to have time to act. In 1999, this was seen in the relatively high nutrient concentration in the near-bottom layers, i.e. from about 70 m up to about 55 m from March to December. As a consequence, a severe summer storm, say, in mid-August, that mixes the water column down to a certain depth, would be more likely to replenish the upper layer with nutrients. But there was no such storm, so the bulk of the water column remained depleted, and was not fully replenished with nutrients until mid-October (when the windy period starts). However, winds were strong enough in the first half of October to replenish the full water column with abundant nutrients. Even if the storms deepen the mixed layer, but insufficiently to reach deep enough down into the lower nutrient-rich layer, no new blooms will be initiated.

The phytoplankton concentration was determined by the interaction of all the processes given in eq. (3) in Part 1. Hence, the phytoplankton concentration did not automatically match the pattern of primary production intensity, although primary production was the dominant process, determining the pattern of phytoplankton concentrations. Fig. 3c therefore shows that, during spring, although primary production was more or less restricted to the upper 15–20 m, the phytoplankton biomass was distributed nearly evenly throughout the 30 m ($Phyt > 200$). The phytoplankton biomass reached mean maximum values from c. 430 mgC m^{-3} in the upper 10 m layer to c. 5 mgC m^{-3} at this depth during the spring bloom. The highest value (c. 580 mgC m^{-3}) was recorded at the sea surface in

the second half of April. Here, the spring bloom had begun in mid-March. This situation was due to the high nutrient concentrations and high daily global radiation in the last ten days of March and in the second half of April. These parameters were used for calculating the primary production, which is the dominant process, determining the phytoplankton biomass pattern. The phytoplankton biomass was low in summer from June till August, most likely as a result of the faster depletion of nutrients and the high phytoplankton grazing by zooplankton. In autumn, there was a slight rise in the phytoplankton biomass; $\{Phyt\}$ remained stable, at a level slightly higher than in summer. This may have been caused by the considerable reduction in the amount of zooplankton, as well as the increase in nutrient concentrations resulting from the deeper mixing of the water. However, the growing season ended in December, when the phytoplankton biomass dropped to the January-February level. The phytoplankton biomass decreased with depth. The greater biomass of phytoplankton in the deeper layers, observed mainly in spring and autumn, was due primarily to sinking algae. The value of $\{Phyt\}$ in the deepest of the layers studied (50–70 m) peaked c. two weeks after the phytoplankton biomass in the upper layer had started to increase.

The growth of the microzooplankton was correlated exactly with that of the phytoplankton (Fig. 3f). Generally speaking, the numbers of microzooplankton in the upper layer were the largest, when the algal biomass there was large. The microzooplankton biomass exhibited two characteristic peaks during the year: the first during the spring bloom, and the second, a small one, in late summer and early autumn. The winter biomass of microzooplankton in the upper layer was c. 0.7 mgC m^{-3}. A considerable increase in Z_{micro} took place in April, shortly after the beginning of the spring bloom. The microzooplankton biomass ranged from 1 to 30 mgC m^{-3} in the spring; in summer, it dropped to < 10 mgC m^{-3} with the concurrently falling phytoplankton biomass, reappearing in early autumn with a higher biomass. The highest biomass of microzooplankton ($Z_{micro} > 20$ mgC m^{-3}) was recorded in the euphotic layer and below it, down to about 30 m depth. Below this depth, the microzooplankton biomass was the lowest. The changes in the microzooplankton biomass in the different layers were conspicuous in that the biomass peaked in the upper layer in May, and subsequently at ever increasing depths. This situation was caused by the occurrence of a greater phytoplankton biomass in these layers.

In this work the biomass of mesozooplankton (*P. elongatus* for stages C1 to adult) was subject to distinct seasonal changes. Fig. 3g illustrates the simulated profiles of *P. elongatus* biomass in the Gdańsk Deep. The biomass peaked in late June – early July, attaining values higher by one

order of magnitude than in winter. At this time, the *P. elongatus* biomass actually reached maximum values of c. 5 mgC m^{-3}. In the first half of the year, the increase in *P. elongatus* biomass was due mainly to the rates of growth and mortality, and to egg production. The calculations indicate clearly, that as food concentrations reach high levels ($\{Phyt\} >$ 250 mgC m^{-3}), the growth rate tends to become constant (the expression $f(\{Phyt\}) = \{Phyt\} - \{Phyt\}_o)/(\{Phyt\} - \{Phyt\}_o + k_{Phyt}) \rightarrow 1$) (see Dzierzbicka-Głowacka 2005a). During the spring bloom the growth rate of *P. elongatus* reached a maximum; however, in May and September it decreased to 70% and 40% respectively. The average mortality rate was obtained on the basis of experimental data given by Klein Breteler et al. (1995) as a function of temperature and food concentration (Dzierzbicka-Głowacka 2005a). The mortality rate in spring depends mainly on food concentration, i.e. it decreases with increasing phytoplankton biomass; however, the effect of temperature is more evident in summer, i.e. mortality increases with rising temperatures. The mortality rate has a substantial influence on the number of females as well as on the number of eggs. The decrease in the numbers of females, due to the mortality rate increasing as a result of rising temperatures, causes egg production to fall (Dzierzbicka-Głowacka 2005a). Predation, determined from the predator biomass (early juvenile herring), becomes apparent during the second half of the year. The increase in predation resulting from the higher predator biomass as a consequence of the faster growth rate, leads to a fall in prey concentration. Vertical migration in the day-night cycle becomes apparent, when prey rises to the upper layer late in the day, and sinking to the lower layer in the morning (Dzierzbicka-Głowacka 1994). In this model the mesozooplankton biomass varies with time because the total biomass of *P. elongatus* is the algebraic sum of the products of the weights W_i and numbers Z_i of 6 cohorts.

The distributions in Figs 4 and 5 present the changes in values of weights W_i and numbers Z_i of six cohorts of *P. elongatus*, including all development stages in the upper and lower layer. In winter, the weights and numbers of individuals decreased slightly owing to the lack of food and the low mortality. In spring, the individual animals became active and grew by feeding on the phytoplankton bloom; the females produced eggs. In the upper layer the development of one distinct generation (the 6th cohort of the 2nd generation) took seven months to complete, from mid-April to mid-November. Individuals of the 3rd generation were produced in November by the females of the 6th cohort of the 2nd generation as a result of the phytoplankton biomass increasing in September; but for lack of food they developed no farther than stage N3. In the lower layer, a complete generation did not develop during the year. The development time for older

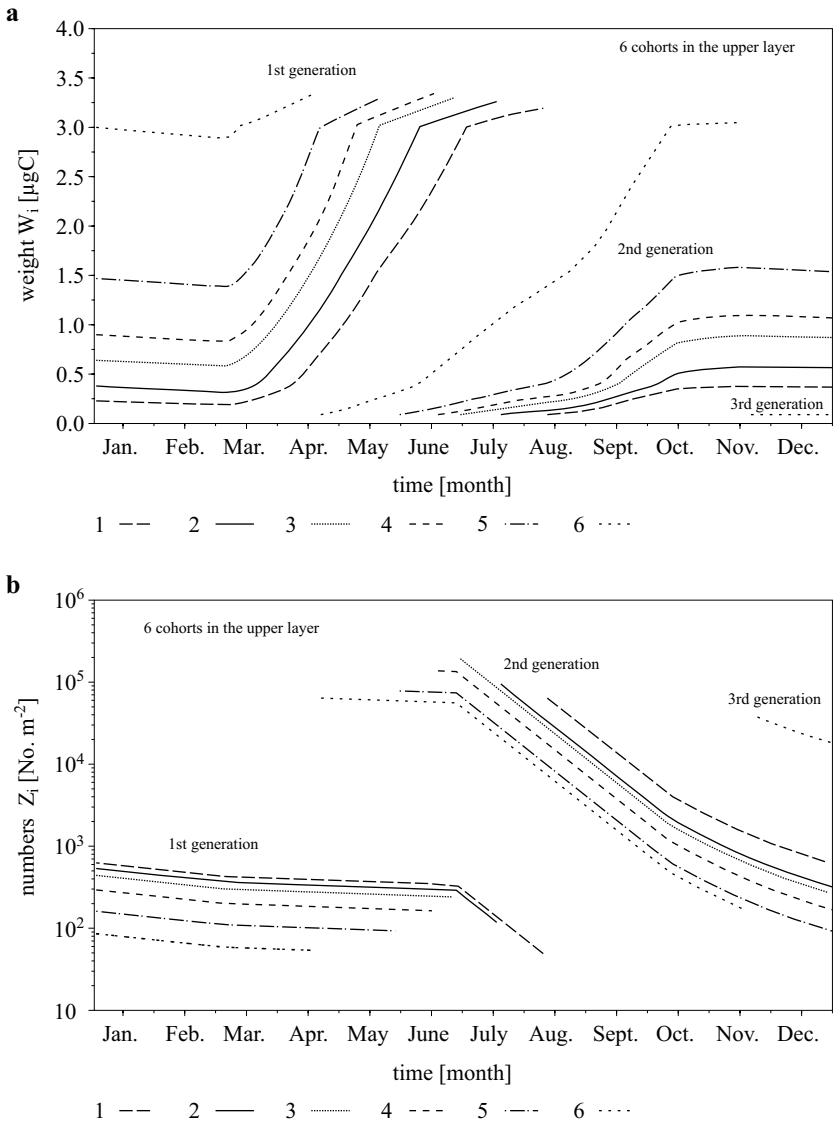

Fig. 4. *Pseudocalanus elongatus.* Weights W_i (a) and numbers Z_i (b) of six cohorts in the upper layer

copepodids was six-seven months; nevertheless, the calculations suggest that a complete generation can develop during a one and a half years. The 1st and 2nd cohorts did not produce any eggs as a result of the considerable decrease in food concentration in the second half of the year.

The predator is represented by early juvenile herring *C. harengus*. The predator growth rate was defined by the encounter rate, which depends on the prey concentration and turbulent encounter velocity as well as the

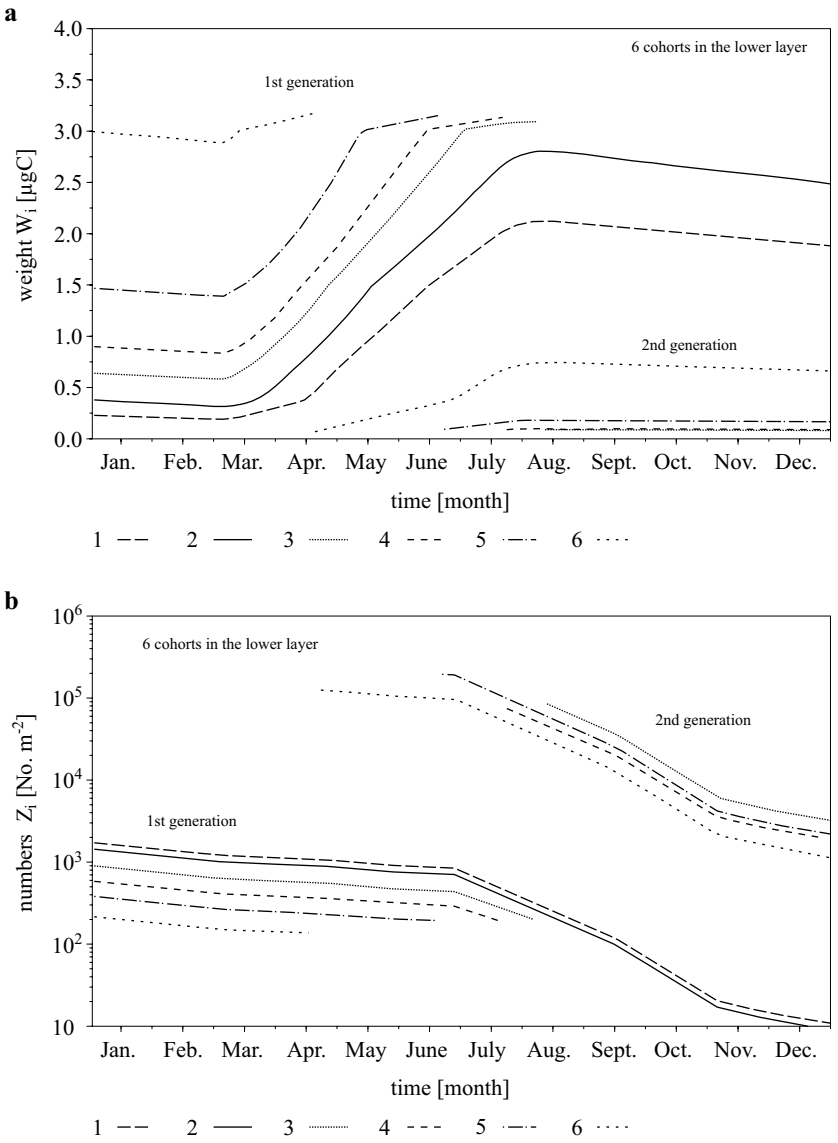

Fig. 5. *Pseudocalanus elongatus*. Weights W_i (a) and numbers Z_i (b) of six cohorts in the lower layer

physiological parameters of the predator. Encounter velocity as a function of dissipation energy depends mainly on the wind speed in the upper layer. However, the mortality rate increases with decreasing prey concentration and at low prey levels is higher than the growth rate.

It was assumed in these calculations that the predator biomass $B = 0$ during the first half of the year and the initial biomass of herring at the end

of June was $B = 28.8$ mgC m^{-3}. The early juvenile herring biomass rose to c. 60 mgC m^{-3} at the end of July, and to 80 mgC m^{-3} at the end of August (Fig. 3h). Another factor contributing to the increase in predator biomass in July and August was the migration of juveniles, i.e. c. 22 in July and 14 mgC m^{-3} in August, from the Vistula Lagoon to the Gdańsk Deep. The biomass of early juvenile herring was highest in late September – early October, attaining a value of c. 100 mgC m^{-3}, when prey concentrations reached their second, lower peak.

5. Discussion

The simulated distributions of the inorganic nitrogen and phosphate concentrations, the surface phytoplankton biomass and depth-integrated biomass of microzooplankton and *P. elongatus* in the model were compared to *in situ* observations from the Gdańsk Deep. Since the outputs of the meteorological submodel were based on meteorological data for 1999, the numerical results were compared to mean values of empirical data for 1999 gleaned from the literature.

The samples of inorganic nitrogen and phosphate taken from the water are given as mean values in the various layers: 0–15 m (euphotic layer, above the seasonal thermocline), 15–30 m (the seasonal thermocline); 30–60 m (the lower part of the seasonal thermocline, the lower part of the isohaline layer) and 60–80 m (the halocline layer). The mean recorded nutrient concentrations in these layers are shown in Fig. 3d for phosphate and Fig. 3e for inorganic nitrogen. The greatest concentrations of phosphate (0.6 mmol m^{-3}) occurred in winter, and the lowest in late spring and summer (June–August) (even $<$ c. 0.01 mmol m^{-3}). In the near-bottom layer, phosphate concentrations were higher than in the upper layer. Maximum concentrations were observed in this layer, where between June and November concentrations above 1.5 mmol m^{-3} were recorded. Concentrations of inorganic nitrogen and phosphate in the upper layer varied according to similar cycles. The highest concentrations were recorded in late winter (March) (6 mmol m^{-3}). The lowest concentrations in the upper layer occurred between May and September and were $<$ c. 0.08 mmol m^{-3}. In the near-bottom layer concentrations of inorganic nitrogen exceeded 10 mmol m^{-3}. Fig. 6a shows the differences between the simulated and mean observed nutrient levels in the upper layer (0–15 m): total inorganic nitrogen – 0.5–1 mmol m^{-3} and phosphate – c. 0.1 mmol m^{-3}. Errors are higher in the near-bottom layer.

The composition and biomass of the main taxonomic groups of phytoplankton were investigated (IMGW 2000). Samples were collected in two layers – 0–10 m and 10–20 m. Among the algae, diatoms and dinoflagellates

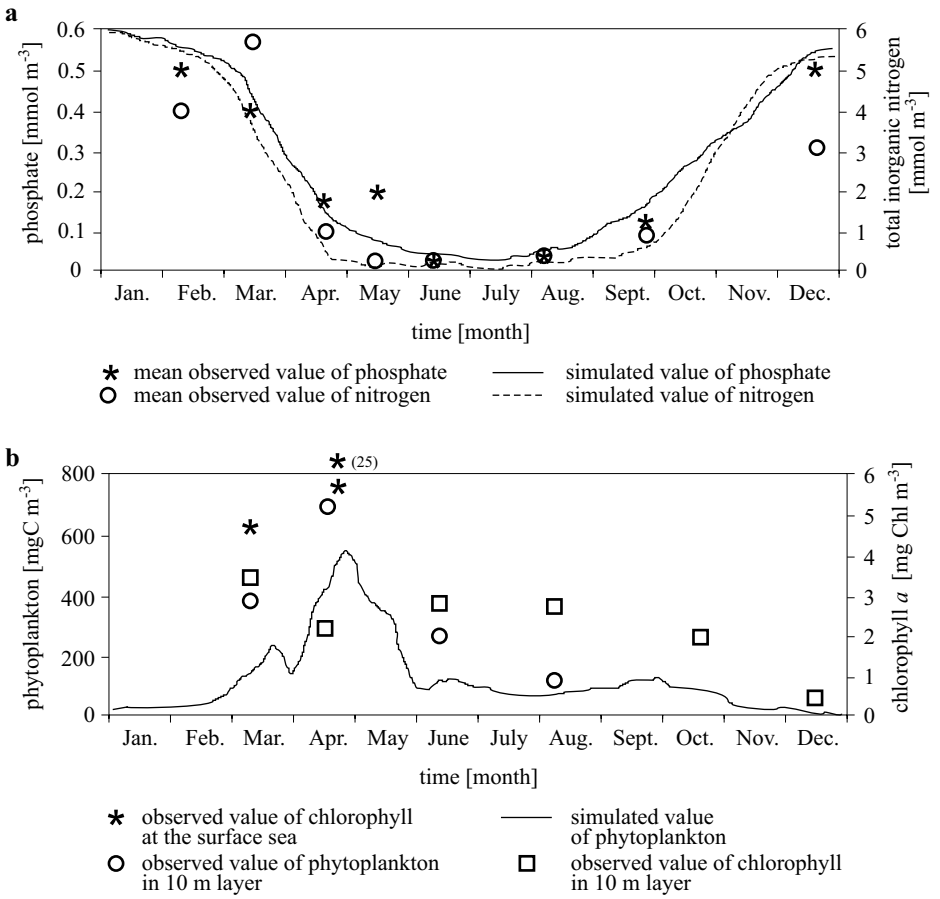

Fig. 6. Simulated and mean observed values of nutrients (a) and phytoplankton and chlorophyll *a* (b) in the upper layer of the Gdańsk Deep in 1999

were present throughout the year. Phytoplankton biomass was high from March to April. The first biomass peak (c. 400 mgC m^{-3}), in March, was dominated by a succession diatom species. In April, the diatom bloom was followed by an intensive bloom of dinoflagellates (c. 700 mgC m^{-3}). In the next period, from June till the autumn, the biomass of algae was not high (Fig. 6b). The phytoplankton biomass is more often measured as chlorophyll *a* than as carbon. Samples of chlorophyll *a* concentration were also collected from these same layers as the phytoplankton. Fig. 6b shows that the first chlorophyll *a* maximum was noted in the upper 10 m layer in March (c. 3.5 mg m^{-3}) and in April (c. 2 mg m^{-3}) in both layers; a second maximum was observed in August (c. 2.5 mg m^{-3}). Surface chlorophyll *a* levels were also obtained by S. Kaczmarek (unpublished data – Regional Oceanographic Database of the Institute of Oceanology PAS).

From the second half of March to the end of April, during the spring bloom, chlorophyll *a* ranged from nearly 3 to about 25 mg m^{-3} in the 30 m layer in the Gdańsk Deep. The mean concentration of chlorophyll *a* was c. 7 mg m^{-3} in the upper 10 m and 5 mg m^{-3} in the 10–30 m layer; however, a very high concentration (c. 25 mg m^{-3}) was found at the surface in late April. To compare the simulated results for phytoplankton carbon with the available chlorophyll *a* data, a C/Chl *a* ratio has to be assumed for converting the simulated carbon contents to chlorophyll *a*. The mean literature value for the C/Chl *a* ratio lies between 31 for open water in the southern Baltic and 43 in the upper layer of coastal water (see Table 1 in Renk 2000). However, Witek et al. (1993) gives the ratio of the carbon level in phytoplankton to the chlorophyll *a* level in the Gulf of Gdańsk (see Fig. 4.2.4. in Witek et al. 1993): in spring in the surface layer, it was 2–4 times greater than during the remainder of the year. This means that in spring smaller amounts of cellular chlorophyll *a* were sufficient to enable the algae to grow. Thus, in the upper layer (10–30 m), the mean observed values of the chlorophyll *a* content of c. 5 mg m^{-3} corresponds, after Renk (2000), to 155 to 215 mgC m^{-3} and, after Witek et al. (1993), to 110 to 275 mgC m^{-3} in March and April respectively.

However, in the surface 10 m layer in April, the mean chlorophyll *a* content of c. 10 mg m^{-3} corresponds, after Renk (2000), to 310 to 430 mgC m^{-3} and, after Witek et al. (1993), to 550 mgC m^{-3}. The highest chlorophyll content of c. 25 mg m^{-3} in April corresponds, after Renk (2000), to 775 to 1075 mgC m^{-3} and, after Witek et al. (1993), to 1375 mgC m^{-3}. The chlorophyll data and the simulated phytoplankton biomass are correlated well enough and attain their maximum concentrations in April, which are of a similar magnitude, depending on the C/Chl *a* conversion factor. In this paper, the calculations were made assuming the C/Chl *a* ratio to be the mean value for the southern Baltic Sea in the upper layer (after Witek et al. 1993), because with this ratio, the values obtained most resemble the observed phytoplankton biomass. Then, the differences in the $\{Phyt\}$ between the modelled and mean observed values are c. 5–25%, depending on the month for which the calculations were made.

Fig. 3f demonstrates the simulated profiles of microzooplankton biomass $\{Z_{micro}\}$. The $\{Z_{micro}\}$ reached maximum values from c. 35 mgC m^{-3} in the upper layer to 1 mgC m^{-3} at the sea bed. High mean microzooplankton biomass was reported in the upper layer in spring (April–May) 1987 – c. 380 $mg_{w.w.}$ m^{-3} (i.e. 200 $mg_{w.w}$ m^{-3} for heterotrophic dinoflagellates and 180 $mg_{w.w}$ m^{-3} for ciliates), which corresponds to c. 46 mgC m^{-3}. The microzooplankton biomass decreased with depth but in the 15 m – bottom layer the biomass peak appeared about two months later than

in the upper layer. This later occurrence of biomass peaks in deeper layers is probably associated with the corresponding changes in feeding conditions at the particular depths. Below a depth of 30 m dinoflagellates from the genus *Gyrodinium* dominated; it is believed that they feed in a phagotrophic manner. Little is known, however, about the quality and size of food particles, feeding rate, and many other aspects of the biology of heterotrophic dinoflagellates (Witek et al. 1993).The copepod nauplii appearing in the upper layer (20 m) only at the end of winter and spring were dominant (in May) in 1987: c. 150 $mg_{w.w}$ m^{-3} (when *Phyt* is high), which corresponds to 9.6 mgC m^{-3}. This is a relatively high biomass, of the order of 1/10 of the biomass of all copepods appearing during the summer (late June – early July). However, the mean biomass of copepod nauplii obtained in 1999 (see IMGW 2000), i.e. in March – c. 6, April – c. 17, June – c. 11 and August – c. 2 $mg_{w.w}$ m^{-3}, which corresponds to 0.38, 1.09, 0.7 and 0.13 mgC m^{-3} respectively. This suggests that the nauplia biomass in 1999 was c. 10 times lower than in 1987. The calculated biomass of microzooplankton is c. 20% lower than that observed in the upper layer in 1987.

P. elongatus occurred in the Gdańsk Deep in great abundance; in deeper layers, below 30 m, it was the dominant species of the mesozooplankton, and below the isohaline layer almost its sole representative. The temporal variability of *P. elongatus* obtained here is shown in Fig. 3g. On the basis of *in situ* data for 1987 (Witek et al. 1993), the biomass of *P. elongatus* in the upper layer of the Gdańsk Deep peaked in late spring (June; c. 200 $mg_{w.w.}$ m^{-3}); in the lower layer, however, it peaked in late July – early August (c. 400 $mg_{w.w.}$ m^{-3}). This corresponds to 13 mgC m^{-3} and 26 mgC m^{-3} respectively. The modelled biomass of *P. elongatus* is half the values given by Witek et al. (1993). This is due mainly to the fact that the mean weights of *P. elongatus* for the development stages used by Witek et al. (1993) and used in the present work, were c. 40% higher than those given by Hernroth (ed.) (1985). However, the mean biomass of copepods (8 species) in the whole water column in the Gdańsk Deep was obtained for 1999 (see IMGW 2000): March – c. 20, April – c. 45, June – c. 80 and August – c. 100 $mg_{w.w}$ m^{-3}, which corresponds to 1.3, 2.9, 5.1 and 6.4 mgC m^{-3}. However, the mean biomass of *P. elongatus* calculated here was 0.1, 0.9, 2.4 and 2.2 mgC m^{-3} in March, April, June and August respectively. Hence, the calculations suggest that the total biomass of *P. elongatus* amount to 30% of the total copepod biomass in the Gdańsk Deep in 1999. Plankton material was also collected (100 μm Copenhagen net) on 20–25 May 1999 in diurnal cycles from the water column, which was divided into several layers. Every single sample was prepared and analysed according to standard HELCOM

methods. Numbers of *P. elongatus* for specific development stages were obtained by Mudrak (2004). During this period, the vertical distributions of observed *P. elongatus* biomass in diurnal cycles were different, i.e. 0.07–0.8 mgC m^{-3} in the upper layer and 0.1–0.9 mgC m^{-3} in the lower one. The average biomass in the whole water column at this time was 0.73 mgC m^{-3}. However, the observed mean values of the depth-integrated biomass were 18.6 and 29.4 mgC m^{-2}; they are therefore half the magnitude of the values obtained here, i.e. c. 40 and 60 mgC m^{-2} at the end of May in the upper and lower layers respectively.

The results here obtained are higher than the ones given by Mudrak (2004). This is probably due to predation, which was assumed to be zero during the first half of year because the predator biomass was equal to zero at this time. The high biomass calculated for May is due to the excessively high initial numbers of adults (the 6th cohort of the 1st generation), which produced too many eggs in April, the low mortality rate in the spring, and the low food ingestion threshold causing an early increase in weight. This situation could also have been caused by migration, which, in this model, was assumed the same for all development stages. According to Mudrak (2004), the youngest development stages (nauplii) were usually found in subsurface layers (mostly between 10 and 20 m). They did not normally change their positions in the water column. Younger copepodids (C1–C2) showed strong diel vertical migration above the halocline, older copepodids (C4–C5) below the thermocline, when adults remained in the deepest part of the water column (near the bottom) (Mudrak et al. 2004). A more detailed comparison between the modelled and observed values has not been possible because no more experimental data for the year in question is available.

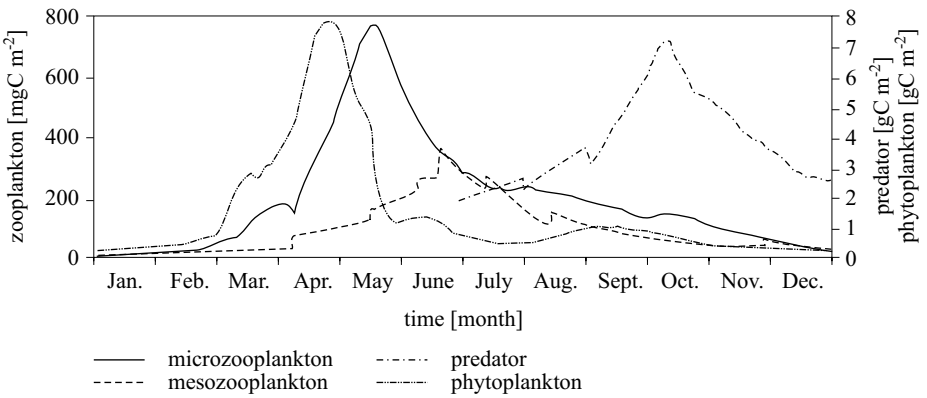

Fig. 7. Simulated depth integrated biomasses of phytoplankton, microzooplankton, mesozooplankton (*Pseudocalanus elongatus*) and early juvenile herring (*Clupea harengus*) in the Gdańsk Deep in 1999

The simulations show the general variations in populations with time (Fig. 7). The results show significant changes in phytoplankton biomass distribution, which took place in an area where there was a considerable increase in primary production. During the spring bloom, there is a substantial growth in phytoplankton biomass, which thereafter falls slightly as a result of the increase in micro- and mesozooplankton biomasses. The microzooplankton biomass reflects the availability of phytoplankton, showing a strong increase with declining food concentrations. However, the later increase in mesozooplankton biomass is caused by the increase in weight of successive cohorts and also in single egg production by each adult. This situation will have led to this substantial growth in the total biomass of *P. elongatus*, which is the algebraic sum of the products of weights W_i and numbers Z_i for stages C1 to adult ($Z_{meso} = \sum W_i \ Z_i$). These small maxima occurring in the distribution Z_{meso} are the result mainly of a single brood by successive cohorts causing their numbers Z_i to increase. Then, the early juvenile herring biomass growth tends to reduce the micro- and mesozooplankton biomasses. An increase in predator biomass depends not only on prey concentration but also on energy dissipation, which in the upper mixed layer is defined by the wind velocity. At low prey levels, the rate of mortality is higher than growth, and there is a decrease in predator biomass.

6. Conclusions

This work presents simulated temporal changes in physical and biological characteristics, i.e. temperature, marine plankton (phytoplankton, micro- and mesozooplankton), early juvenile fish and nutrients (total inorganic nitrogen and phosphate). The numerical simulations were done with the $1D$-Coupled Ecosystem Model, a meteorological, physical and biological model with a high-resolution mesozooplankton (herbivorous copepods) module and a simple the prey-predator model; this was described in Part 1. Such models are suitable as tools for testing hypotheses, as a result of which we can evaluate our understanding of processes and dynamics.

The calculations were done for one station in the Gdańsk Deep in the southern Baltic Sea for one particular year (1999). The results of the numerical simulations described here accord with the *in situ* observations for nutrients and phytoplankton. The modelled and mean observed phytoplankton biomasses differ by 5–25% in the 10 m upper layer and by 30% at the sea surface and depend on the month for which the calculations were made. They also depend on the C/Chl a ratio for converting simulated carbon contents to chlorophyll a. Comparison of the nutrient concentrations from the calculated and mean experimental data

indicates that the difference in $Nutr$ is c. 30% in the lower layer. However, the $Nutr$ in the 15 m upper layer in winter differ by up to 1 mmol m^{-3} (inorganic nitrogen) and up to 0.1 mmol m^{-3} (phosphate), i.e. c. 20%; in the summer, the differences are c. 5%. However, the calculated depth-integrated biomass of *P. elongatus* differs from the mean recorded value by 30–50% at the end of May.

A major problem that now needs to be addressed concerns the quality of the field data used to test such simulations. The problems with such data arise from the fact that the spatial and temporal variability in zooplankton is usually so great that any model with the right orders of magnitude in its outputs will fit the data. So even if we apply models that treat herbivores in some detail, the testing of these models may rest primarily upon the nutrient and phytoplankton levels, which can be measured with greater accuracy.

In summary, the 1D-Coupled Ecosystem Model can be utilised for performing numerical investigations of the temporal changes in nutrient distributions (total inorganic nitrogen and phosphate), and the biomasses of phytoplankton, microzooplankton, *P. elongatus* and early juvenile herring (*C. harengus*).

In my opinion, I have achieved the objective of this work: I have been able to construct a meteorological-physical-biological model for the southern Baltic Sea, coupled with a copepod model and a simple prey-predator model, which is very much more detailed and complex than previous ones. The copepod model for *P. elongatus* links trophic processes and population dynamics and simulates individual growth within 6 cohorts, including successive stages. However, the simple prey-predator model for early juvenile herring *C. harengus* is based on the encounter rate controlled by behavioural and turbulent processes.

The 1DCEM model is a suitable tool for studying the annual, seasonal, monthly and daily variability of marine plankton in the southern Baltic Sea. Hence, it can therefore be applied in the forecasting of ecological changes in the Baltic.

The study the impact of various climatic conditions over several years is the long-term objective of my work. I intend to simulate the seasonal dynamics of another species of mesozooplankton in the Baltic Sea (as *Acartia* spp.) using the model presented in this paper. In the future, I would also like to include in this model additional equations for bacteria and for zoobenthos species and to extend the *prey -predator* model with an equation for the sprat (*Sprattus sprattus*). The Baltic Sea fishery is based to a high degree on planktivorous fish such as the herring (*C. harengus*) and sprat (*S. sprattus*), which feed on herbivorous copepods such as *P. elongatus* and *Acartia* spp.

Acknowledgements

I would like to thank Dr L. Bielecka and Dr S. Mudrak from Gdańsk University and Dr S. Kaczmarek from the Institute of Oceanology for providing the experimental data.

References

Apel J. R., 1987, *Principles of ocean physics*, Int. Geophys. Ser., Vol. 38, Acad. Press, London, 631 pp.

Billen G., Lancelot C., Maybeck M., 1991, *N, P and Si retention along the aquatic continuum from land to ocean*, [in:] *Ocean margin processes in global change, physical, chemical, and earth sciences research*, R. F. C. Mantoura, J. M. Martin & R. Wollast (eds.), Wiley & Sons, New York, 19–44.

Blaxter J. H. S., Holliday F. G. T., 1963, *The behavior and physiology of herring and other clupeids*, Adv. Mar. Biol., 1, 261–393.

Czyszek W., Wensierski W., Dera J., 1979, *Solar radiation energy inflow and absorption in the Baltic water*, Sci. Comm. Ocean. Res., 26, 105–140.

Dzierzbicka-Głowacka L., 1994, *Numerical analysis of the influence of grazing on the two-dimensional distribution function of the phytoplankton concentration in a stratified sea*, Oceanologia, 36 (2), 155–173.

Dzierzbicka-Głowacka L., 2005a, *A numerical investigation of phytoplankton and Pseudocalanus elongatus dynamics in the spring bloom time in the Gdańsk Gulf*, J. Marine Syst., 53 (1)–(4), 19–36.

Dzierzbicka-Głowacka L., 2005b, *Modelling the seasonal dynamics of marine plankton in southern Baltic Sea. Part 1. A Coupled Ecosystem Model*, Oceanologia, 47 (4), 591–619.

Dzierzbicka-Głowacka L., 2006, *Encounter rate in plankton*, Pol. J. Environ. Stud., 15 (2), 243–257.

Edler L. (ed.), 1979, *Recommendation on methods of marine biological studies in the Baltic Sea. Phytoplankton and chlorophyll*, Baltic Mar. Biol. Publ. No 5, 1–38.

Fey D. P., 2001, *Differences in temperature conditions and somatic growth rate of larval and early juvenile spring-spawned herring from the Vistula Lagoon, Baltic Sea manifested in the otolith to fish size relationship*, J. Fish. Biol., 58 (8), 1257–1273.

Frost B. W., 1989, *A taxonomy of the marine calanoid copepod genus Pseudocalanus*, Can. J. Zool., 67 (3), 525–551.

Gill A. E., 1982, *Atmosphere-ocean dynamics*, Int. Geophys. Ser., Vol. 30, Acad. Press, 662 pp.

Hernroth L. (ed.), 1985, *Recommendations on methods for marine biological studies in the Baltic Sea. Mesozooplankton biomass assessment*, Baltic Mar. Biol. Publ. No 10, 1–32.

Johannessen A., Blom G., Folkvord A., 2000, *Differences in growth pattern between spring and autumn spawned herring (Clupea harengus L.) larvae*, Sarsia, 85, 461–466.

Klein Breteler W. C. M., Gonzales S. R., Schogt N., 1995, *Development of Pseudocalanus elongatus (Copepoda, Calanoida) cultured at different temperature and food conditions*, Mar. Ecol. Prog. Ser., 119, 99–110.

Kremer J. N., Nixon S. W., 1978, *A coastal marine ecosystem. Simulation and analysis*, Ecol. Stud., Vol. 24, Springer-Verlag, Heidelberg, 219 pp.

Launiainen J., 1979, *Studies of energy exchange between the air and the sea surface on the coastal area of Gulf of Finland*, Fin. Mar. Res., 246, 3–110.

Lehman A., 1995, *A three-dimensional baroclinic eddy-resolving model of the Baltic Sea*, Tellus, 47 (A), 1013–1031.

Margoński P., 2000, *The abundance, growth rate and mortality of the early life stages of herring (Clupea harengus) and smelt (Osmerus eperlanus) in the Vistula Lagoon (southern Baltic Sea) during 1998–1999*, ICES CM 2000/N:21.

IMGW, 2000, *Environmental conditions in the Polish zone of the southern Baltic Sea during 1999*, Oddz. Mor. Inst. Meteorol. Gosp. Wod., Gdynia, (in Polish with English summary).

Miller T. J., Crowder L. B., Rice J. A., Marshall E. A., 1988, *Larval size and recruitment mechanisms in fishes: toward a conceptual framework*, Can. J. Fish. Aquat. Sci., 45, 1657–1670.

Mudrak S., 2004, *Short- and long-term variability of zooplankton in coastal Baltic water using the Gulf of Gdańsk as an example*, Ph. D. dissertation, Univ. Gdańsk, Gdynia, 323 pp., (in Polish).

Mudrak S., Bielecka L., Żmijewska M. I., 2004, *Diel vertical migrations of copepoda from the Gdańsk Deep (Baltic Sea)*, 39th Europ. Mar. Biol. Symp., Genoa 2004, (abstracts).

Parsons T. R., Tokahashi M., Hargrave B., 1984, *Biological oceanographic processes*, 3rd edn., Pergamon Press, Oxford, 330 pp.

Postma H., Rommets J. W., 1984, *Variations of particulate organic carbon in the central North Sea*, Nether. J. Sea Res., 18, 31–50.

Radach G., Berg J., Heinemann B., Krause M., 1984, *On the relation of primary production and herbivorous zooplankton grazing in the northern North Sea during FLEX'76*, [in:] *Flows of energy and materials in marine ecosystems, theory and practice*, M. Fasham (ed.), NATO Conf. Ser., Vol. 4, Plenum Press, New York, 597–625.

Radach G., Moll A., 1993, *Estimation of the variability of production by simulating annual cycles of phytoplankton in the central North Sea*, Prog. Oceanogr., 31, 339–419.

Renk H., 2000, *Primary production in the southern Baltic*, Stud. Mater. Mor. Inst. Ryb. (Gdynia), 35 (A), 78 pp., (in Polish).

Rozwadowska A., Isemer H.-J., 1998, *Solar radiation fluxes at the surface of the Baltic Proper. Part 1. Mean annual cycle and influencing factors*, Oceanologia, 40 (4), 307–330.

Steele J. H., 1974, *The structure of marine ecosystems*, Harvard Univ. Press, Cambridge, 12 pp.

Sundby S., Fossum P., 1990, *Feeding conditions of Arcto-Norwegian cod larvae compared with the Rothschild-Osborn theory on small-scale turbulence and plankton contact rates*, J. Plankton Res., 12 (6), 1153–1162.

Sverdrup H. U., 1953, *On conditions for the vernal blooming of phytoplankton*, J. Cons. Perm. Int. Explor. Mer, 18, 287–295.

Varela R. A., Cruzado A., Gabaldom J. E., 1995, *Modelling primary production in the North Sea using the European Regional Seas Ecosystem Model*, Nether. J. Sea Res., 33 (3/4), 337–361.

Viitasalo M., Flinkman J., Viherluoto M., 2001, *Zooplanktivory in the Baltic Sea: a comparison of prey selectivity by Clupea harengus and Mysis mixta, with reference to prey escape reactions*, Mar. Ecol. Prog. Ser., 216, 191–200.

Vinogradov M. E., Shushkina E. A., 1987, *Functioning of pelagic plankton communities in the euphotic zone of the ocean*, Nauka, Moskva, 240 pp., (in Russian).

Witek Z., 1995, *Biological production and its consumption in the marine ecosystem of the western Gdańsk Basin*, Wyd. Mor. Inst. Ryb., Gdynia, 145 pp., (in Polish).

Witek Z., Bralewska J., Chmielewski H., Drgas A., Gostkowska J., Kopacz M., Knurowski J., Krajewska-Sołtys J., Lorenz Z., Maciejewska K., Mackiewicz T., Nakonieczny J., Ochocki S., Warzocha J., Piechura J., Renk H., Stopiński M., Witek B., 1993, *Structure and function of marine ecosystem in the Gdańsk Basin on the basis of studies performed in 1987*, Stud. Mater. Oceanol., 63, 5–125.

Zapadka T., Woźniak S. B., Woźniak B., 2001, *A simple formula for the net long-wave radiation flux in the southern Baltic Sea*, Oceanologia, 43 (3), 265–277.

Appendix

Table 1. Dynamical constants, variables, and conversion factors in the biological submodel

Symbol	Value	Unit	Meaning	Reference
B	variable	mgC m^{-3}	predator biomass	
d_A	variable	gC(gChl h)$^{-1}$	assimilation number	
d_I	variable		light limitation factor	
d_P	variable		limitation factor of phosphate	
d_N	vaiable		limitation factor of total inorganic nitrogen	
d	variable	cm	predator reaction distance	
d_o	variable	mm	body length of predator	
$\{Detr\}$	variable	gCm^{-2}	detritus concentration	
E_o	variable	W m^{-2}	photosynthetically available irradiation PAR	
E_{opt}	variable	kJ m^{-2} h^{-1}	saturation irradiance	
E	variable	kJ m^{-2} h^{-1}	irradiance at depth z	
E	variable	s^{-1}	encounter rate	
f_{max}	0.17	day^{-1}	maximum growth rate for Z_{micro}	author after Witek (1995)
g_{max}	0.5	day^{-1}	maximum grazing rate	Radach et al. (1984)
g_N	0.0167	mmol N(mgC)$^{-1}$	N/C ratio	Varela et al. (1995)
g_P	0.612×10^{-3}	mmol P(mgC)$^{-1}$	P/C ratio	Varela et al. (1995)
g_{Chl}	variable	gC(gChl a)$^{-1}$	C/Chl a ratio	Witek et al. (1995)
g_B	variable	day^{-1}	predator growth rate	
g_1	10^{-6}		proportionality parameter between growth rate and encounter rate	Dzierzbicka-Głowacka (2006)
g_2	0.02	day^{-1}	constant growth rate term	Dzierzbicka-Głowacka (2006)
k_{Nutr_N}	0.05	mmol N m^{-3}	half-saturation constant for total inorganic nitrogen	Varela et al. (1995)
k_{Nutr_P}	0.06	mmol P m^{-3}	half-saturation constant for phosphate	Radach et al. (1984)
k_{Phyt}	100	mgCm^{-3}	half-saturation constant for grazing	Radach & Moll (1993)
K_z	variable	m^2s^{-1}	turbulent diffusion ceffi-cient	

Table 1. (*continued*)

Symbol	Value	Unit	Meaning	Reference
l	variable	m	characteristic length scale of turbulent eddies	
m_P^n	0.1		percentage of basic respiration	Parson et al. (1984)
m_P^d	0.05		percentage of photorespiration	Parson et al. (1984)
m_P	0.05	day^{-1}	mortality rate of $\{Phyt\}$	Radach & Moll (1993)
m_Z	variable	day^{-1}	mortality rate of $\{Z_{meso}\}$	
n_e	0.33		percentage of ingestion regenerated as soluble excretion of zooplankton	Steele (1974)
n_f	0.33		percentage of ingestion egested as faecal material	Steele (1974)
n_z	0.33		percentage of ingestion ending up as dead zooplankton	Steele (1974)
$\{Nutr\}_N$	variable	$\mathrm{mmol\,N\ m}^{-3}$	total inorganic nitrogen	
$\{Nutr\}_P$	variable	$\mathrm{mmol\,P\ m}^{-3}$	phosphate concentration	
p_f	0.2		percentage of remineralised faecal material in the water column	Postma & Rommets (1984)
p_p	0.2		percentage of remineralised dead organic matter in the water column	Postma & Rommets (1984)
p_z	0.2		percentage of remineralised dead zooplankton in the water column	Postma & Rommets (1984)
$\{Phyt\}_0$	10	mgCm^{-3}	phytoplankton grazing threshold	Radach et al. (1984)
$\{Phyt\}$	variable	$\mathrm{mgC\ m}^{-3}$	phytoplankton biomass	
r_d	0.0167	day^{-1}	remineralisaton rate of benthic detritus	Billen et al. (1991)
t_1	0.621		temperature coefficient	obtained by autor
t_2	1.1		temperature coefficient	Kremer & Nixon (1978)
w	variable	$\mathrm{m\ s}^{-1}$	encounter turbulent velocity	
W_{female}	52	$\mu\mathrm{g}_{w.w}$	female weight	Hernroth (ed.) (1985)
W_{egg}	0.3	$\mu\mathrm{g}_{d.w}$	egg weight	Frost (1989)
W_i	variable	μgC	weights of i cohorts	
Z_i	variable	m^{-3}	numbers of i cohorts	
$\{Z_{micro}\}$	variable	$\mathrm{mgC\ m}^{-3}$	microzooplankton biomass	

Table 1. (*continued*)

Symbol	Value	Unit	Meaning	Reference
$\{Z_{meso}\}$	variable	mgC m^{-3}	mesozooplankton biomass	
X	0.8		efficiency term	L. Bielecka (pers. comn.)
τ	1		coefficient of food selection	the author
ε	variable	m^{2}s^{-1}	dissipation rate of turbulent kinetic energy	

Table 2. Dynamic constants and variables in the physical submodel

Symbol	Value	Unit	Meaning	Reference
A_z	variable	m^2 s^{-1}	turbulent diffusion coefficient	
c	1.0	kcal kg^{-10} C^{-1}	specific heat of sea water for 8°C	Gill (1982)
f	1.230×10^{-4}	s^{-1}	Coriolis parameter	Apel (1987)
T	variable	°C	temperature	
T_o	4	°C	initial temperature	IMGW (2000)*
U_{10}	variable	m s^{-1}	wind velocity	
u	variable	m s^{-1}	water velocity in the x-direction	
v	variable	m s^{-1}	water velocity in the y-direction	
Q_g	variable	W m^{-2}	global radiation	
Q_B	variable	W m^{-2}	back radiation	
Q_L	variable	W m^{-2}	latent heat flux	
Q_S	variable	W m^{-2}	sensible heat flux	
τ_x	variable	kg s^{-2}	wind stress in the x-direction	
τ_y	variable	kg s^{-2}	wind stress in the y-direction	
ρ_o	10^3	kg m^{-3}	density of water at 4°C	Gill (1982)
ρ	variable	kg m^{-3}	water density	

* Maritime Branch Materials, IMGW (2000).